

Performance of coal-based activated carbon modified with NiFe_2O_4 for raw water treatment

Subroto¹, Muhammad Said² , Eddy Ibrahim³ , Poedji Loekitowati Hariani^{4*} 

¹ Doctoral Program, Environmental Science, Universitas Sriwijaya, Jl. Padang Selasa, Palembang, 30139, Indonesia

² Department of Chemical Engineering, Faculty of Engineering, Universitas Sriwijaya, Jalan Palembang-Prabumulih, Indralaya, Ogan Ilir 30862, Indonesia

³ Department of Mining Engineering, Faculty of Engineering, Universitas Sriwijaya, Jalan Palembang-Prabumulih, Indralaya, Ogan Ilir 30862, Indonesia

⁴ Department of Chemistry, Faculty of Mathematics and Natural Sciences, Universitas Sriwijaya, Jalan Palembang-Prabumulih, Indralaya, Ogan Ilir 30862, Indonesia

* Corresponding author's e-mail: puji_lukitowati@mipa.unsri.ac.id

ABSTRACT

This study evaluates the effectiveness of an activated carbon/ NiFe_2O_4 composite in the treatment of raw water from the Lematang River, with an emphasis Fe, Mn, and turbidity levels. Activated carbon is produced through the treatment of coal with a KOH activator. The characterization of activated carbon and the activated carbon/ NiFe_2O_4 composite involved X-ray diffraction (XRD), (BET) surface area analysis, scanning electron microscopy with energy dispersive X-ray (SEM-EDX), vibrating sample magnetometer (VSM), and fourier transform-infrared spectroscopy (FTIR). The surface area of activated carbon/ NiFe_2O_4 composite is 293.992 m^2/g and demonstrates magnetic properties, indicated by a saturation magnetization value of 21.13 emu/g. The optimal conditions for the removal of Fe, Mn, and turbidity were determined to be a dosage of 0.4 g/L, a contact time of 60 min, and a stirring speed of 250 rpm. Under optimal conditions, the composite demonstrated a significant removal efficiency for Fe (96.12%), Mn (98.78%), turbidity (87.02%), TSS (93.49%), and COD (59.27%), along with an increase in pH from 5.38 to 7.66. The Langmuir adsorption isotherm is the appropriate adsorption model to reduce Fe, Mn and turbidity. Activated carbon/ NiFe_2O_4 composite exhibits significant potential for applications in clean water provision.

Keywords: activated carbon, NiFe_2O_4 , composite, raw water, adsorption.

INTRODUCTION

Water contamination refers to the introduction of unwanted substances into a water body, which significantly impacts its quality and leads to detrimental consequences for the environment and human well-being. Current water resources have been affected by several variables including climate change, population expansion, heightened human activity, agricultural practices, and industrial operations. The provision of drinking water is a significant concern, particularly in developing nations [Hoslett et al., 2018; El-Alfy et al., 2019]. An essential factor in assessing the development level of a country is the accessibility of potable

water for both household and industrial use [Majdi et al., 2019; 4. García-Avila et al., 2021].

The water from the Lematang River serves as a primary source of raw water to meet the clean water needs of the residents of Muara Enim Regency, located in South Sumatra, Indonesia. Raw water contains various metal ions dissolved from soil and rocks, including iron (Fe), manganese (Mn), copper (Cu), and zinc (Zn), which may come from natural processes or human activities. However, the most important metal ions to remove from raw water are Fe and Mn. These two metals, when present in high concentrations, can cause water quality issues, such as a metallic taste, unpleasant odor, and discoloration of

the water to brown or black. High levels of total suspended solids (TSS), turbidity, Fe, and Mn pose challenges when using raw water for drinking. These parameter levels frequently exceed the threshold, particularly during the wet season due to colloidal particles in the size range of 1 nm to 1 μm . Meanwhile, efficient removal of high-turbidity water by sedimentation or filtration has limitations [Chiavola et al., 2023].

Drinking water industries have employed aluminium sulphate (alum) treatment on raw water to decrease these characteristics. Alum is the primary chemical coagulant widely employed in water treatment to reduce turbidity and color. However, its use leads to the formation of alum residues and the generation of sludge [Koul et al., 2022; Ameh et al., 2024]. The presence of excessive alum in drinking water can have detrimental impacts on human health, particularly when it accumulates over an extended period. Water treatment supposedly aims to produce clear, safe, colorless and odorless water, which is used to meet the clean water needs of the community. The adsorption technology is noted for its affordability, ease of use, high performance, efficiency, stability, and effective regeneration in the removal of water pollutants [Abdelhamid et al., 2020; Qasem et al., 2021].

Activated carbon is a promising adsorbent for the detection and removal of contaminants from river water. Activated carbon possesses significant pore structures and a defined surface area [Njewa et al., 2022]. Activated carbon can be produced from a range of carbon-rich materials, including palm shells [Kittappaa et al., 2020], agricultural waste [Mollaei et al., 2024], walnut shells [Shabir et al., 2024], coconut shells [Saad, 2024], and bamboo stems [Bakara et al., 2024]. Coal is a potential raw material for activated carbon. Lower-grade coal is frequently less appealing to power plant because of its poor calorific value and elevated concentration of impurities such as water, oxygen, and ash [Altintig et al., 2022; Musa et al., 2024]. However, through appropriate processing methods, low-grade coal can be transformed into activated carbon. Coal-based activated carbon is more affordable, readily available, and has superior surface characteristics [Shaida et al., 2022]. Indonesia has a large coal supply, with the majority of production concentrated in South Sumatra, where the research was conducted.

The application of activated carbon as an adsorbent is subject to several constraints,

particularly during separation. Magnetic activated carbon, a modification of porous carbon with magnetic materials, is recognized as a highly promising separation process [Cazetta et al., 2016]. The approach offers a significant benefit because the resulting composite has a robust structure, allowing for straightforward separation of both composite and the adsorbed pollutants using a simple external magnet. Furthermore, it is capable of being recycled and reused [Liu et al., 2017; Fourotan et al., 2019]. Several researchers have synthesized magnetic activated carbon for specific applications, such as ceftriaxone adsorption using activated carbon- Fe_3O_4 [Badi et al., 2018], Methyl red dye adsorption using activated carbon- MnFe_2O_4 [Riyanti et al., 2018], H_2S removal using ZnFe_2O_4 /activated carbon [Yang et al., 2020], and ciprofloxacin adsorption using activated carbon- MgFe_2O_4 [Huynh et al., 2023].

This study aimed to synthesize activated carbon from coal and modify it with nickel ferrite (NiFe_2O_4). Subsequently, the activated carbon/ NiFe_2O_4 composite was utilized to decrease the Fe, Mn, and turbidity levels in water from the Lematang River. KOH is used as an activator in the production of activated carbon from coal. KOH plays a role in suppressing tar formation, speeds up the removal of non-carbon elements, and increases the rate of pyrolysis reactions. This process leads in the production of numerous pores and pore volumes, which eventually increases surface area [Jawad and Abdulhameed., 2020; Mi et al., 2024]. NiFe_2O_4 is characterized by its excellent chemical stability, strong coercivity, moderate saturation magnetization, high electrical resistivity, and abundant natural availability [Chetia et al., 2024; Mousa et al., 2021]. NiFe_2O_4 possesses magnetic properties that enable the composite to be more easily separated from the liquid medium by applying an external magnetic field once the adsorption process is finished [Hariani et al., 2022]. The combination of the adsorptive properties of activated carbon and the magnetic properties of NiFe_2O_4 makes this composite highly efficient in water purification.

MATERIAL AND METHODS

Materials

The chemicals used in this study were nickel (II) chloride hexahydrate (>98%), iron (III)

chloride hexahydrate (>99%), potassium hydroxide, iron (III) standard solution 1000 ppm, Manganese (II) standard solution 1000 ppm, and sodium hydroxide purchased from Merck, Germany and deionized water was used as a solvent. Coal from the coal mine in Tanjung Enim regency, whereas raw water was taken from the Lematang River, Muara Enim regency, South Sumatra, Indonesia.

Activated carbon preparation

Activated carbon was synthesized using the procedures outlined by Liu et al. [2024] and Mi et al. [2024]. After removing impurities, the coal was oven-dried for 24 h at 105 °C. Subsequently, the coal was ground to a particle size of 140 mesh. A total of 50 g of coal powder was then immersed in a 1 M KOH solution at a weight ratio of 1:2. The coal, saturated with the KOH solution for 1 h, was then heated in an oven for 24 h at 105 °C. Subsequently, the sample was subjected to carbonation at a temperature of 600 °C with a flow rate of 5 °C/min, using N₂ gas for 2 h. The sample was rinsed with deionized water until it reached a neutral pH. The activated carbon was subsequently desiccated at a temperature of 105 °C for 2 h and ultimately sealed in a glass receptacle. The moisture and ash content of the activated carbon were analyzed according to the Indonesian National Standard [SNI 06-3730-1995].

The synthesis of activated carbon/NiFe₂O₄ composite

The synthesis of an activated carbon/NiFe₂O₄ composite was conducted using the coprecipitation technique as described by Bernaoui et al. [2022] and Kazi et al. [2023]. An equal mass of 4 g of activated carbon, 5.41 g of FeCl₃·6H₂O and 2.38 g of NiCl₂·6H₂O (with a molar ratio of Fe³⁺ and Ni²⁺ of 2:1) were combined in 25 mL of deionized water. The solution was stirred and gradually immersed in a 2 M NaOH solution until it reached a pH of approximately 10, under the influence of N₂ gas. The composite material was rinsed with deionized water until it reached a neutral pH and then dried at 105 °C for an additional 3 h. Finally, calcination was conducted at 450 °C for 3 h.

Characterization of materials

Activated carbon and activated carbon/NiFe₂O₄ composites were characterized by X-ray

diffraction (XRD Rigaku Miniflex 300 Japan), Cu Ka radiation, wavelength λ=1,541.862 Å, in the range of 2θ = 10-90°. The Brunauer-Emmett-Teller (BET) measurement was performed to assess the surface area of the samples, utilizing a Micromeritics volumetric instrument (NOVA Touch 4LX) with an N₂ adsorption/desorption isotherm system. scanning electron microscopy – energy dispersive X-ray (SEM-EDX JEOL JSM-6510LA) was employed to investigate the surface morphology and elements of the samples. The examination of magnetic characteristics aimed to determine the magnetic properties of the materials using a vibrating sample magnetometer (VSM-7307). The identification of functional groups was achieved by Fourier transform infrared spectroscopy employing KBr pellets in the wave number range of 400–4000 cm⁻¹ (Perkin Elmer FTIR-1650).

Characterization of raw water

Water samples were collected at the inlet of the Lematang River before entering the raw water reservoir (Figure 1). Prior to usage, the sample bottles underwent cleaned and sterilized. The water samples were collected in polyethylene plastic bottles and kept in an ice box at a temperature of 4 °C during collection and transport. The initial measurements were total Fe and Mn concentrations, pH, chemical oxygen demand (COD), turbidity, and total suspended solid (TSS). The analysis adhered to the requirements set by APHA/AWWA/WEF [2017].

Adsorption

Activated carbon and activated carbon/NiFe₂O₄ composites were employed for the reduction of Fe, Mn, and turbidity in samples of raw water. The aforementioned parameter is considered to establish the optimal removal conditions. The adsorption procedure was conducted using batch adsorption, with the following variables: dosage ranging from 0.2 to 0.7 g/L, contact time ranging from 30 to 150 min, and stirring speed between 100 and 400 rpm. The percentage efficiency was calculated using the following formula:

$$\text{Removal (\%)} = \frac{(C_0 - C_t)}{C_0} \times 100 \quad (1)$$

where: C₀ and C_t are initial concentration and concentration at any given time.

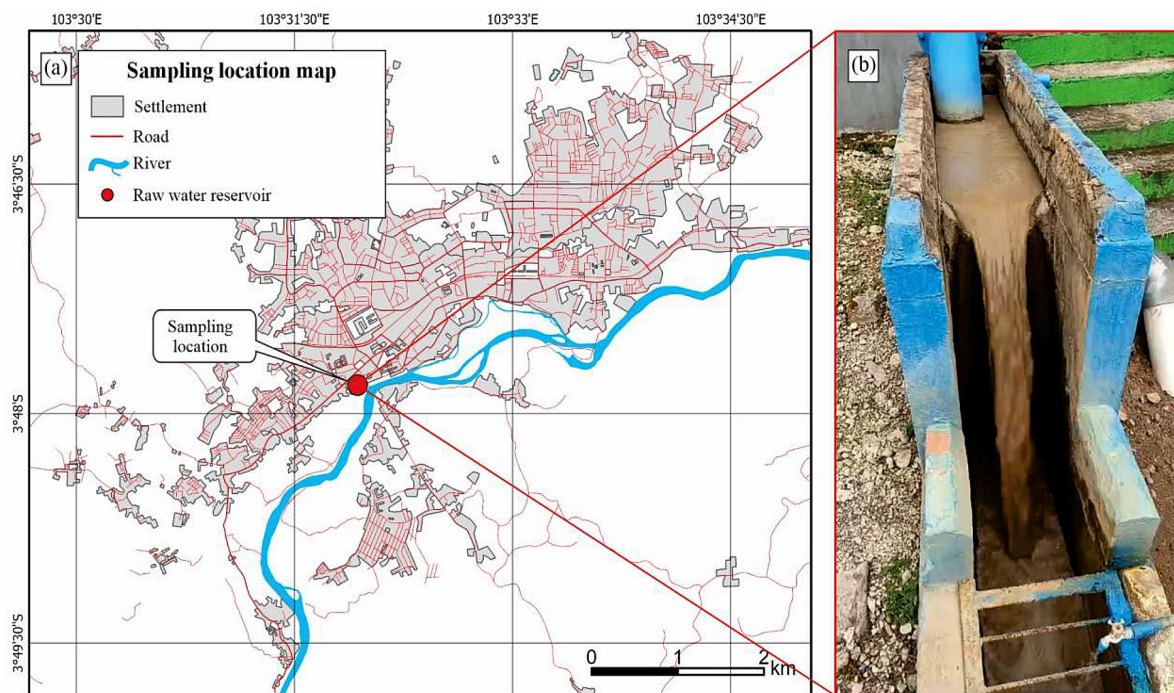


Figure 1. (a) Sampling location map, and (b) inlet of the Lematang River into the raw water reservoir

RESULTS AND DISCUSSION

Characterization of activated carbon and activated carbon/ NiFe_2O_4 composite

Table 1 shows the results of the analysis of moisture and ash content in activated carbon. The moisture and ash content of activated carbon comply with the provisions of the Indonesian National Standard (SNI No. 06-3730-1995) for activated carbon. Increased moisture leads to the saturation of activated carbon pores by water, therefore limiting the accessible area for adsorbing pollutant molecules. Ash content refers to the proportion of inorganic substances (non-carbon particles) present in activated carbon. Ash may be derived from either minerals or contaminants. An elevated ash level can disrupt the adsorption process and induce undesired reactions.

Figure 2 displays the XRD patterns of activated carbon and the activated carbon/ NiFe_2O_4 composite. Two distinct diffraction peaks of activated carbon, associated with the Miller indices (002) and (100), are detected at around 22° and 44° , respectively. The peaks observed are associated

with the amorphous structure of the disordered aromatic groups [Frohlich et al., 2019; Bakara et al., 2024]. The diffraction patterns of the activated carbon/ NiFe_2O_4 composite shows peaks at $2\theta = 30.11^\circ, 35.01^\circ, 36.12^\circ, 43.11^\circ, 54.01^\circ, 57.08^\circ,$ and 63.12° which corresponds to the crystal plane of (220), (311), (222), (400), (422), (511), and (440). These crystal planes can be classified as inverse spinel NiFe_2O_4 with face-centered cubic (FCC) structural arrangement [JCPDS Card No. 10-0325]. Due to the more crystalline structure of NiFe_2O_4 compared to activated carbon, the XRD patterns of the activated carbon/ NiFe_2O_4 composite do not exhibit the amorphous characteristics. It is consistent with the findings of Azzam et al. [2023], on which the biochar/ NiFe_2O_4 composite exhibits a single peak corresponding to NiFe_2O_4 . The absence of foreign peaks indicates that the structure is a homogeneous single phase.

The porosity characteristics of activated carbon and activated carbon/ NiFe_2O_4 composites were determined by examining the N_2 adsorption-desorption isotherms and BET surfaces shown in Figure 3. IUPAC categorizes it as a type IV

Table 1. Moisture and ash content of activated carbon

Parameters	Percentage (%)	SNI (%)
Moisture	8.22	Max. 15
Ash content	1.90	Max. 10

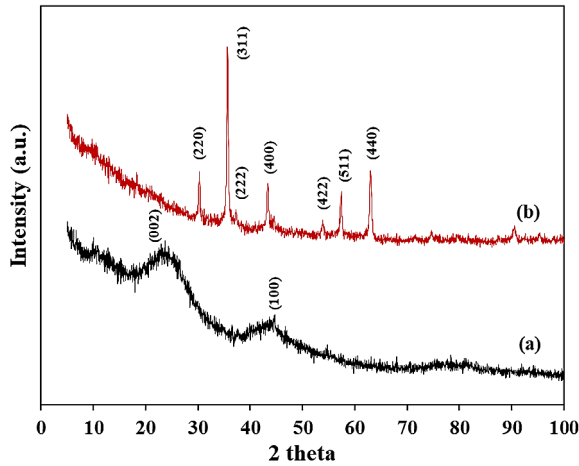


Figure 2. XRD spectra of (a) activated carbon and (b) activated carbon/NiFe₂O₄ composite

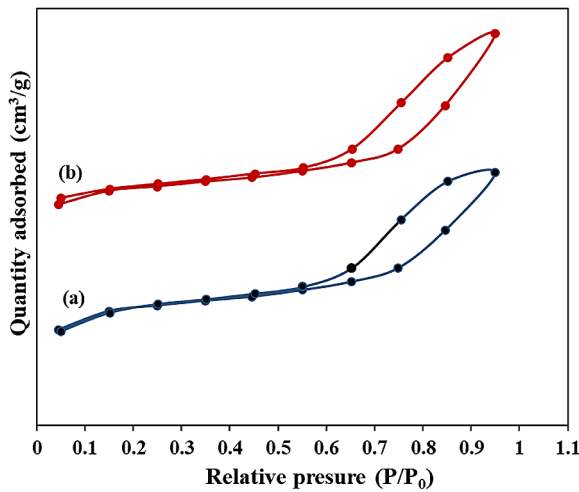


Figure 3. N₂ adsorption-desorption isotherms of (a) activated carbon and (b) activated carbon/NiFe₂O₄ composite

isotherm that falls within the P/P₀ range of 0.5–1.0, suggesting the presence of many mesoporous structures [Sun et al., 2023]. The activated carbon/NiFe₂O₄ composite has a surface area of 293.992 m²/g larger than the activated carbon (Table 2). The results of a similar study by other researchers showed that activated carbon derived from *Sargassum oligocystum* biomass and walnut shells exhibited a smaller surface area compared

to activated carbon-Fe₃O₄ composites [Foroutan et al., 2019; Tahmasebpour and Peighambar-doust, 2024]. Fe₃O₄ can either enlarge the existing pores in the activated carbon or generate new microstructures, which has the potential to increase the overall surface area due to the formation of smaller and additional pores.

Figure 4 displays an SEM image of activated carbon and the activated carbon/NiFe₂O₄ composite. The activated carbon surface appears to have pores, albeit not uniformly distributed. Meanwhile, the activated carbon/NiFe₂O₄ composite surface indicates that a portion of the NiFe₂O₄ is dispersed on the activated carbon surface. EDX analysis suggests that the primary element of activated carbon is C (93.89%), with O (6.11%) accounting for the remaining quantity. Fe and Ni in the activated carbon/NiFe₂O₄ composite show that the synthesis went well (Table 3).

Figure 5 depicts a curve of magnetization versus applied magnetic field for activated carbon/NiFe₂O₄ composites. The composites demonstrate superparamagnetic characteristics, as evidenced by a saturation magnetization value of 21.13 emu/g. This magnetic characteristic enhances the efficiency of separation following the adsorption process. This study reports a saturation magnetization that surpasses 16.21 emu/g of activated carbon derived from hazelnut shells, produced by hydrothermal impregnation with NiFe₂O₄ [Livani et al., 2018]. Meanwhile, the saturation magnetization value of NiFe₂O₄ is 32.9 emu/g [Abbas et al., 2023]. The addition of activated carbon reduces the concentration of magnetic components in the composite, so the magnetic intensity decreases.

Batch equilibrium studies

Fe, Mn, and turbidity levels are used as parameters to examine the optimal conditions for treating raw water. Analysis of raw water reveals that the concentrations of Fe, Mn, and turbidity are 5.68 mg/L, 3.29 mg/L, and 51.6 NTU, respectively. To reduce the previously discussed parameter, a series of adsorption experiments are conducted involving three variables: dosage,

Table 2. The pore structure of activated carbon and activated carbon/NiFe₂O₄ composite

Characteristics	Activated carbon	Activated carbon/NiFe ₂ O ₄ composite
BET surface area (m ² /g)	265.443	293.992
Average pore diameter (nm)	3.697	3.673
Pore volume (cm ³ /g)	0.217	0.266

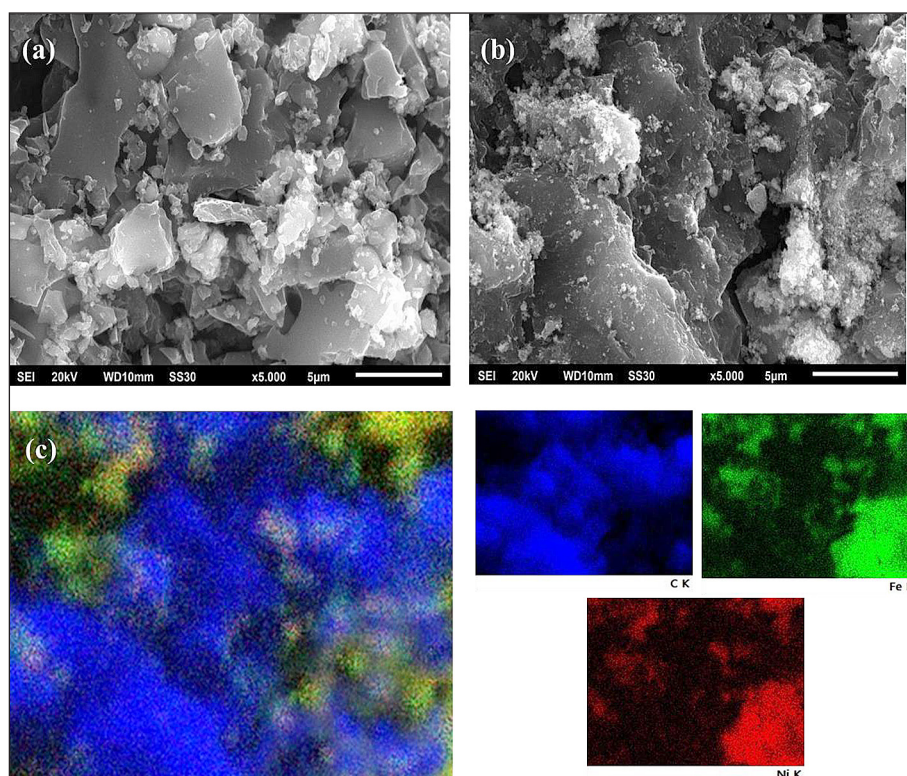


Figure 4. SEM image of (a) activated carbon, (b) activated carbon/ NiFe_2O_4 composite, and (c) mapping activated carbon/ NiFe_2O_4 composite

Table 3. Elemental of activated carbon and activated carbon/ NiFe_2O_4 composite

Element (%)	Activated carbon	Activated carbon/ NiFe_2O_4 composite
C	93.89	61.06
O	6.11	25.97
Fe	–	8.82
Ni	–	4.15

contact time, and stirring speed. The adsorbent dosage used varies within 0.2–0.7 g/L. The data presented in Figure 6a demonstrates that as the dosage increases, the number of adsorption sites on the adsorbent surface also increases, therefore enabling a greater amount of pollutants to be absorbed. Additional dosages do not correspondingly improve the rate of elimination, which suggests a saturation point for the adsorption [Badawi et al., 2024]. Activated carbon and activated carbon/ NiFe_2O_4 composites overall exhibit a comparable tendency to reduce Fe and Mn. The increase with the increasing dosage of the adsorbent and subsequently plateau after the optimal dosage is reached. However, the activated carbon/ NiFe_2O_4 composite appears more effective than activated carbon alone. The maximum removal achieved by the activated carbon/ NiFe_2O_4 composite is

0.4 g/L, while using activated carbon results in a higher dosage of 0.5 g/L.

Figure 6b shows how contact time affects the ability of activated carbon and activated carbon/ NiFe_2O_4 composites to reduce Fe, Mn and turbidity. The contact time ranges from 30 to 150 min. The optimal contact time required to achieve equilibrium in activated carbon is greater than in activated carbon/ NiFe_2O_4 composite. The activated carbon/ NiFe_2O_4 composite achieved equilibrium within 60 min, with removal efficiencies of 87.12% for Fe, 94.85% for Mn, and 77.52% for turbidity, respectively. Meanwhile, the optimal contact time for activated carbon was 120 min with lower removal percentages. The combination of activated carbon and NiFe_2O_4 not only enhances the separation process but also augments the adsorption capacity. Another investigation

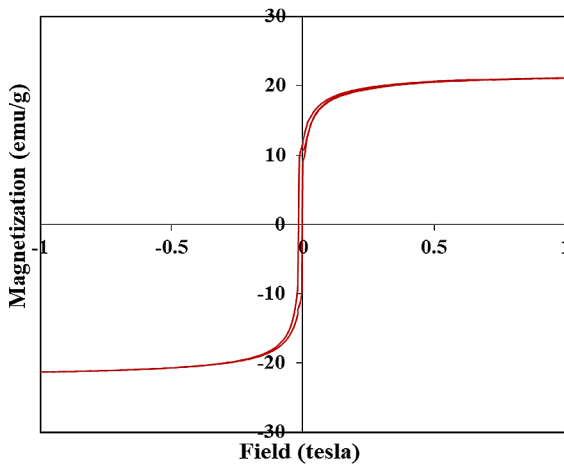


Figure 5. VSM curve of activated carbon/ NiFe_2O_4 composite

demonstrated that the adsorption of Cd using activated carbon/ Fe_3O_4 was superior to solely activated carbon [Vaithianathan et al., 2023].

Figure 6c illustrates the impact of varying stirring speeds on the removal efficiency of activated carbon and the activated carbon/ NiFe_2O_4 composite in reducing Fe, Mn, and turbidity. The stirring speed varies between 100 and 400 rpm. The findings suggest that reduced stirring speed corresponds to less effective elimination of pollutants, owing to inadequate dispersion for the thorough mixing of the adsorbent and contaminants [Badawi et al., 2024]. Increased stirring speed result in enhanced mass transfer from the solution to the surface of the adsorbent. The reason is that stirring improves external diffusion, specifically the transport of molecules from the liquid phase to the adsorbent’s surface, which facilitates a greater number of dissolved molecules to reach the activated carbon or composite surface. The optimal stirring speed was achieved with an activated carbon/ NiFe_2O_4 composite at 250 rpm, compared to 300 rpm when using activated carbon. Additionally, the activated carbon/ NiFe_2O_4 composite consistently showed superior performance in removing Fe, Mn, and turbidity compared to activated carbon alone at similar stirring speeds.

The findings of the study suggest that the activated carbon/ NiFe_2O_4 composite exhibits superior efficacy in pollutant reduction. The combined use of activated carbon and NiFe_2O_4 leads to an increased quantity of active sites, exhibited by enhanced physical and chemical characteristics. The activated carbon/ NiFe_2O_4 composite possesses a larger surface area compared to pure activated

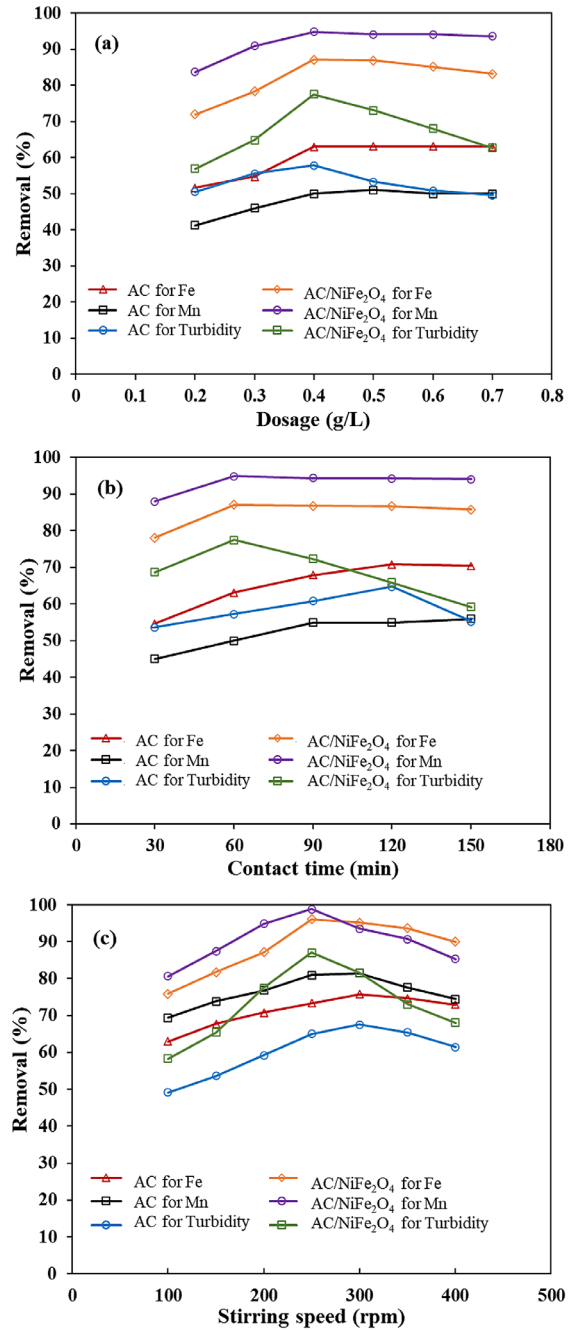


Figure 6. Effect of (a) dosage, (b) contact time, and (c) stirring speed of activated carbon (AC) and activated carbon/ NiFe_2O_4 composite for removal Fe, Mn and turbidity

carbon. The magnetic properties of NiFe_2O_4 help attract Fe ions through magnetic interactions, improving the binding of Fe ions on the composite surface more effectively than pure activated carbon, which relies solely on its physical adsorption properties. The optimal condition of activated carbon/ NiFe_2O_4 composite was reached at a dosage of 0.4 g, a contact time of 60 min, and a stirring speed of 250 rpm. Meanwhile, activated carbon

Table 4. The physicochemical characteristics of the raw water before and after treatment using activated carbon/ NiFe_2O_4 composite

Parameters	Before	After	Removal (%)	Quality standards
Fe (mg/L)	5.68	0.22	96.12	Max. 1.0
Mn (mg/L)	3.29	0.04	98.78	Max. 0.5
Turbidity (NTU)	51.60	6.70	87.02	Max. 25
TSS (mg/L)	3.230	210	93.49	Max. 1000
COD (mg/L)	356	145	59.27	–
pH	5.38	7.66	–	6.5–8.5

reached its optimum condition at a dosage of 0.5 g, contact time of 120 min, and stirring speed of 300 rpm. Table 4 provides the measurements of Fe, Mn, turbidity, TSS, COD, and pH in raw water prior to and following the application of the activated carbon/ NiFe_2O_4 composite. All parameters in raw water exceed the established quality criteria. Following the application of the activated carbon/ NiFe_2O_4 composite, there is a reduction in these values and satisfying the clean water criteria for sanitation purposes. According to the Regulation of the Minister of Health of Indonesia No. 32 of 2017 for Hygiene and Sanitation, the Environmental Health quality standards for water sources are as follows: maximum turbidity level of 25 NTU, TSS limit of 1000 mg/L, pH range of 6.5–8.5, Fe and Mn limits of 1.0 mg/L and 0.5 mg/L, respectively.

The activated carbon/ NiFe_2O_4 composite shows better performance in enhancing water quality compared to previous studies. The modified nano-banana peel powder achieved reductions in turbidity (83%), TSS (73.8%), and COD

(31.7%) in river water from Valli Aaru, India [Dharsana and Prakash, 2023]. Activated carbon from sawdust was used to enhance wastewater quality, resulting in a pH change from 7.7 to 7.10 and a reduction in TSS from 232 mg/L to 15.7 mg/L (93.23%) [Oladimeji et al., 2021]. *Moringa oleifera* seed powder was utilized for treating domestic wastewater in Zomba, Malawi, reducing turbidity from 287 NTU to 38.8 NTU (86.48%) and increasing the pH from 4.3 to 7.1 [Vunain et al., 2019]. Manganese green sand used in acid mine water treatment can reduce Fe and Mn by 69.94% and 70.61%, respectively [Kusdarini et al., 2023]. Figure 7 illustrates the color difference in raw water before and after the addition of the activated carbon/ NiFe_2O_4 composite, where the originally cloudy raw water becomes noticeably clearer following the adsorption process.

Adsorption isotherm

The Langmuir and Freundlich isotherms are mathematical models used to describe the adsorption process. The Langmuir isotherm assumes that adsorption occurs on a homogeneous surface with a limited number of adsorption sites while the Freundlich isotherm describes adsorption on a heterogeneous surface [Detho et al., 2021]. The linearity of the Langmuir and Freundlich isotherm equation is expressed as follows:

$$\frac{C_e}{q_e} = \frac{1}{b \cdot Q_m} - \frac{C_e}{Q_m} \quad (2)$$

$$\log q_e = \log K_f + \frac{1}{n} \log C_e \quad (3)$$

where: q_e represents the amount of adsorbate per gram of adsorbent at equilibrium (mg/g), Q_m denotes the maximum adsorption capacity (mg/g), and C_e indicates the concentration of adsorbate at equilibrium (mg/L). The parameter n reflects the



Figure 7. Raw water before and after treatment using activated carbon/ NiFe_2O_4 composite

adsorption intensity, while b and K_f are constants specific to the Langmuir and Freundlich models, respectively.

Table 5 provides the adsorption isotherm parameters of an activated carbon/NiFe₂O₄ composite for Fe, Mn, and turbidity. The Langmuir isotherm better represents the adsorption model, as indicated by the R^2 value being closer to 1 compared to the Freundlich isotherm. A similar pattern is observed in the adsorption of Pb, Cd, and Ni from Jakarta River water using iron oxide [Ameh et al., 2024]. The Langmuir isotherm effectively describes monolayer adsorption on a homogeneous surface.

Reusability of activated carbon/NiFe₂O₄ composite

The study of the reusability of activated carbon/NiFe₂O₄ composite is a very important aspect because the efficiency of using adsorbents has an impact on reducing costs significantly. Reusability was carried out to evaluate the stability of activated carbon/NiFe₂O₄ composite to reduce Fe, Mn and turbidity in five cycle. This process is carried out by separating the activated carbon/NiFe₂O₄ composite from the solution after use using an external magnet, then soaking it in 0.1 M HCl for 30 min. The precipitate was separated from the solution, washed with ethanol and distilled water and finally dried using an oven at a temperature of 80 °C for 10 h. Figure 8 demonstrates the strong recyclability of the activated carbon/NiFe₂O₄ composite, with Fe, Mn, and turbidity removal efficiencies of 93.22%, 95.25%, and 82.15% even after 5 cycles. In addition, the magnetic properties of a material minimize the risk of damage to the material surface thereby increasing adsorption efficiency [Kalidason and Kuroiwa, 2022].

FTIR spectra

This study employed FTIR spectroscopy to analyze the alterations in functional groups of the activated carbon/NiFe₂O₄ composite following its application in raw water treatment. Figure 8 presents three FTIR spectra: activated carbon, activated carbon/NiFe₂O₄ composite, and activated carbon/NiFe₂O₄ composite post-adsorption. The OH functional group is evident in all three spectra, observed as a broad absorption peak at wave numbers approximately 3300–3400 cm⁻¹. The peak corresponds to the stretching vibration of water molecules adsorbed on carbon, carboxyl, or hydroxyl surfaces. The wave number at 1600 cm⁻¹ is associated with the bending vibration of water molecules or the asymmetric stretching vibration of the C=O group in carboxylate compounds. The wide peak observed at 1020 cm⁻¹ corresponds to the C-O stretching vibration of the activated carbon framework [Badawi et al., 2024; Atiyah et al., 2024]. The FTIR spectrum between 400 and

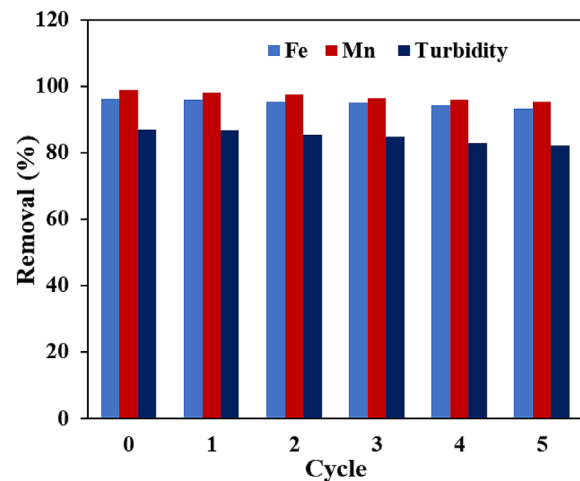


Figure 8. Reusability of activated carbon/NiFe₂O₄ composite

Table 5. Adsorption isotherm parameters for removal Fe, Mn and turbidity

Adsorption isotherm parameters	Adsorbate		
	Fe	Mn	Turbidity
Langmuir			
R^2	0.9976	0.9969	0.9971
b (L/mg)	0.376	0.337	0.277
Q_m (mg/g)	58.82	52.910	47.39
Freundlich			
R^2	0.9831	0.9876	0.9775
K_f (g/mg.min)	14.45	11.96	9.70
n	1.518	1.389	1.006

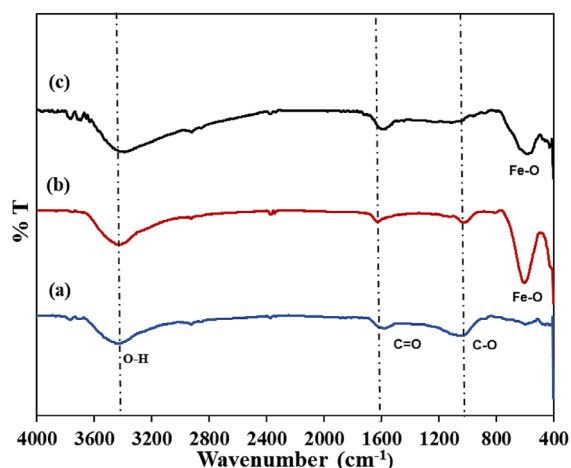


Figure 9. FTIR spectra of (a) activated carbon, (b) activated carbon/ NiFe_2O_4 composite and (c) activated carbon/ NiFe_2O_4 composite after adsorption

700 cm^{-1} is attributed to the stretching vibration of metal-oxygen bonds [Hazarika et al., 2018]. The wave number of 599 cm^{-1} in the activated carbon/ NiFe_2O_4 composite indicates a tetrahedral characteristic of NiFe_2O_4 , specifically the Fe-O group. The FTIR spectrum of the post-use activated carbon/ NiFe_2O_4 composite shows a variation in spectral intensity sharpness, this suggests a bond exists between the metal ion and the adsorbent [Kasirajan et al., 2022]. It can be seen that the absorption band of the Fe-O bond in the composite weakens after the adsorption process occurs.

CONCLUSIONS

This study investigates the application of activated carbon/ NiFe_2O_4 composite in the treatment of raw water, aiming to serve as a resource for clean water supply within the community. Activated carbon is produced from coal and subsequently modified with NiFe_2O_4 through the coprecipitation method. The moisture and ash content of activated carbon comply with the quality standards established by the Indonesian National Standard. The activated carbon/ NiFe_2O_4 composite demonstrates superior performance relative to activated carbon and exhibits magnetic properties, enabling separation from the solution using a magnet. The optimal treatment was achieved at a dosage of 0.4 g , a contact time of 60 min , and a stirring speed of 250 rpm . Under these conditions, the removal efficiencies attained were as follows: Fe at 96.12% , Mn at 98.78% , turbidity

at 87.02% , TSS at 93.49% , and COD at 59.27% . Additionally, the pH value improved from 5.38 to 7.66 . The treatment of raw water from Lematang River with an activated carbon/ NiFe_2O_4 composite achieves compliance with sanitation water quality standards. The activated carbon/ NiFe_2O_4 composite demonstrates high stability, with less than 5% decrease in removal efficiency observed after five cycles. This research establishes a foundation for future clean water supply treatment in developing nations.

Acknowledgements

This research is funded by the Directorate of Research, Technology, and Community Service of the Directorate General of Higher Education, Research and Technology in accordance with the Implementation Contract for the State University Operational Assistance Program for the 2024 Fiscal Year Research Program No. 090/E5/PG.02.00.PL/2024 under the Doctoral Dissertation Research scheme.

REFERENCES

1. Abbas Z.M.A., Shatti W.A., Kareem M.M., Khodair Z.T. (2023). Synthesis and characterization of $\text{NiFe}_2\text{O}_4/\text{CuO}$ nanocomposites: Structural and magnetic properties analysis. *Chemical Data Collections*, 47, 1-15. <https://doi.org/10.1016/j.cdc.2023.101078>
2. Abdelhamid A.E., El-Sayed A.A., Khalil A.M. (2020). Polysulfone nano functionalized grapheme oxide for dye removal from wastewater. *Journal of Polymer Engineering*, 40, 833–841. <https://doi.org/10.1515/polyeng-2020-0141>
3. Ameh P.O., Habila M.A., Garg R., Onoyima C.C., Ihegboro G.O., Ononamadu J.C., Garg R., Adamu Z. Joel U.J., Showunmi R. (2024). Removal of contaminants from river Jakara using iron oxide nanoparticles prepared from *Citrullus lanatus* fruit waste. *Journal of Hazardous Materials Advances*, 15, 1–11. <https://doi.org/10.1016/j.hazadv.2024.100450>
4. APHA/AWWA/WEF. (2017). Standard Methods for the examination of water and wastewater. 23rd edition, American Public Health Association, American Water Works Association, Water Environment Federation, Denver.
5. Altintig E., Alsancak A., Karaca H., Angin D., Altundag H. (2022). The comparison of natural and magnetically modified zeolites as an adsorbent in methyl violet removal from aqueous solutions. *Chemical Engineering Communications*, 209, 555–569. <https://doi.org/10.1080/00986445.2021.1874368>

6. Atiyah Z.Y., Muallah S.K., Abbar A.H. (2024). Removal of COD from petroleum refinery wastewater by adsorption using activated carbon derived from avocado plant. *South African Journal of Chemical Engineering*, 48, 467–483. <https://doi.org/10.1016/j.sajce.2024.03.015>
7. Azzam A.B., Tokhy Y.A., El Dars F.M., Younes A.A. (2023). Heterogeneous porous biochar-supported nano NiFe₂O₄ for efficient removal of hazardous antibiotic from pharmaceutical wastewater. *Environmental Science and Pollution Research*, 30, 119473–119490. <https://doi.org/10.1007/s11356-023-30587-5>
8. Badawi A.K., Hassan R., Alghamdi A.M., Ismail B., Osmanf R.M., Salama R.S. (2024). Advancing cobalt ferrite-supported activated carbon from orange peels for real pulp and paper mill wastewater treatment. *Desalination and Water Treatment*, 318, 1–10. <https://doi.org/10.1016/j.dwt.2024.100331>
9. Badi M.Y., Azari A., Pasalari H., Esrafil A., Farzadkia M. (2018). Modification of activated carbon with magnetic Fe₃O₄ nanoparticle composite for removal of ceftriaxone from aquatic solutions. *Journal of Molecular Liquids*, 261, 146–154. <https://doi.org/10.1016/j.molliq.2018.04.019>
10. Bakara I.U., Nurhafizah M.D., Abdullah N., Akinawo O.O., Ul-Hamid A. (2024). Investigation of kinetics and thermodynamics of methylene blue dye adsorption using activated carbon derived from bamboo biomass. *Inorganic Chemistry Communications*, 166, 1–11. <https://doi.org/10.1016/j.inoche.2024.112609>
11. Bernaoui C.K., Bendraoua A., Zaoui F., Gallardo J.J., Navas J., Boudia R.A., Djedjai H. Goual N.E.H., Adjdir M. (2022). Synthesis and characterization of NiFe₂O₄ nanoparticles as reusable magnetic nanocatalyst for organic dyes catalytic reduction: Study of the counter anion effect. *Materials Chemistry and Physics*, 292, 1–11. <https://doi.org/10.1016/j.matchemphys.2022.126793>
12. Cazetta A.L., Pezoti O., Silva T., Junior A.P., Asefa T., Almeida V.C. (2016). Magnetic activated carbon derived from biomass waste by concurrent synthesis: efficient adsorbent for toxic dyes. *ACS Sustainable Chemistry & Engineering*, 4(3), 1058–1068. <https://doi.org/10.1021/acssuschemeng.5b01141>
13. Chetia T., Suleman A., Chetia B. (2024). A comprehensive review on magnetic NiFe₂O₄ nanoparticles: Synthesis approaches and catalytic proficiency in various coupling reactions. *Tetrahedron*, 164, 1–17. <https://doi.org/10.1016/j.tet.2024.134172>
14. Chiavola A., Marcantonio C.D., D'Agostini M., Leoni S., Lazzazzara M. (2023). A combined experimental-modeling approach for turbidity removal optimization in a coagulation–flocculation unit of a drinking water treatment plant. *Journal of Process Control*, 130, 1–10. <https://doi.org/10.1016/j.jprocont.2023.103068>
15. Detho A., Daud Z., Rosli M.A., Ridzuan M.B.B., Awang H. (2021). Reduction of COD and ammoniacal nitrogen from landfill leachate using granular activated carbon and green mussel adsorbent. *Desalination and Water Treatment*, 223, 218–226. <https://doi.org/10.5004/dwt.2021.27140>
16. Dharsana M., Prakash A.J. 2023. Nano-banana peel bio-coagulant in applications for the treatment of turbid and river water. *Desalination and Water Treatment*, 294, 100–110. <https://doi.org/10.5004/dwt.2023.29491>
17. El-Alfy M.A., Hasballah A.F., El-Hamid H.T., El-Zeiny A.M. (2019). Toxicity assessment of heavy metals and organochlorine pesticides in freshwater and marine environments, Rosetta area, Egypt using multiple approaches. *Sustainable Environment Research*, 29, 1–12. <https://doi.org/10.1186/s42834-019-0020-9>
18. Foroutan R., Mohammadi R., Razeghi J., Ramavandi B. (2019). Performance of algal activated carbon/Fe₃O₄ magnetic composite for cationic dyes removal from aqueous solutions. *Algal Research*, 40, 1–12. <https://doi.org/10.1016/j.algal.2019.101509>
19. Frohlich A.C., Foletto E.L., Dotto G.L. (2019). Preparation and characterization of NiFe₂O₄/activated carbon composite as potential magnetic adsorbent for removal of ibuprofen and ketoprofen pharmaceuticals from aqueous solutions. *Journal of Cleaner Production*, 229, 828–837. <https://doi.org/10.1016/j.jclepro.2019.05.037>
20. García-Avila F., Avil'es-Anazco A., Sanchez-Cordero E., Valdiviezo-Gonz'ales L., Ordonez, M.D.T. (2021). The challenge of improving the efficiency of drinking water treatment systems in rural areas facing changes in the raw water quality. *South African Journal of Chemical Engineering*, 37, 141–149. <https://doi.org/10.1016/j.sajce.2021.05.010>
21. Hariani P.L., Said M., Rachmat A., Salni S., Aprianti N., Amatullah A.F. (2022). Synthesis of NiFe₂O₄/SiO₂/NiO Magnetic and application for the photocatalytic degradation of Methyl orange dye under UV irradiation. *Bulletin of Chemical Reaction Engineering & Catalysis*, 17(4), 699–711. <https://doi.org/10.9767/bcrec.17.4.15788.699-711>
22. Hazarika K.K., Goswami C., Saikia H., Borah B.J., Bharali P. (2018). Cubic Mn₂O₃ nanoparticles on carbon as bifunctional electrocatalyst for oxygen reduction and oxygen evolution reactions. *Molecular Catalysis*, 451, 153–160. <https://doi.org/10.1016/j.mcat.2017.12.012>
23. Hoslett J., Massara T.M., Malamis S., Ahmad D., Van den Boogaert I., Katsou E., Ahmad B., Ghazal H., Simons S., Wrobel L., Jouhara H. (2018). Surface water filtration using granular media and

- membranes: a review. *Science of The Total Environment*, 639, 1268–1282. <https://doi.org/10.1016/j.scitotenv.2018.05.247>
24. Huynh N.C., Nguyen T.T.T., Nguyen D.T.C., Tran T.V. (2023). Production of $MgFe_2O_4$ /activated carbons derived from a harmful grass *Cynodon dactylon* and their utilization for ciprofloxacin removal. *Chemosphere*, 343, 1–13. <https://doi.org/10.1016/j.chemosphere.2023.139891>
25. Jawad A.H., Abdulhameed A.S. (2020). Statistical modeling of methylene blue dye adsorption by high surface area mesoporous activated carbon from bamboo chip using KOH-assisted thermal activation. *Energy Ecology and Environment*, 5, 456–469. <https://doi.org/10.1007/s40974-020-00177-z>
26. Kalidason, A., Kuroiwa, T. (2022). Synthesis of chitosan–magnetite gel microparticles with improved stability and magnetic properties: A study on their adsorption, recoverability, and reusability in the removal of monovalent and multivalent azo dyes. *Reactive and Functional Polymers*, 173, 1–9. <https://doi.org/10.1016/j.reactfunctpolym.2022.105220>
27. Kasirajan R., Bekele A., Girma E. (2022). Adsorption of lead (Pb-II) using CaO-NPs synthesized by solgel process from hen eggshell: Response surface methodology for modeling, optimization and kinetic studies. *South African Journal of Chemical Engineering*, 40, 209–229. <https://doi.org/10.1016/j.sajce.2022.03.008>
28. Kazi, S., Inamdar, S., Sarnikar, Y., Kamble, D., Tigote, R. (2023). Simple Co-precipitation synthesis and characterization of magnetic spinel $NiFe_2O_4$ nanoparticles. *Materials Today*, 73(3), 448–454. <https://doi.org/10.1016/j.matpr.2022.09.590>
29. Kittappaa S., Jaisa F.M., Ramalingam M., Mohd N.S., Ibrahim S. (2020). Functionalized magnetic mesoporous palm shell activated carbon for enhanced removal of azo dyes. *Journal of Environmental Chemical Engineering*, 8(5), 1–10. <https://doi.org/10.1016/j.jece.2020.104081>
30. Koul B., Bhat, N., Abubakar, M., Mishra, M., Arukha, A.P., Yadav, D. (2022). Application of natural coagulants in water treatment: a sustainable alternative to chemicals. *Water*, 14(22), 1–27. <https://doi.org/10.3390/w14223751>
31. Kusdarini E., Sania P.R., Budianto A. (2023). Adsorption of iron and manganese ions from mine acid water using manganese green sand in batch process. *Journal of Ecological Engineering*, 24(12), 158–166. <https://doi.org/10.12911/22998993/173007>
32. Liu B., Lv P., Wang Q., Bai Y., Wang J., Su W., Song X., Yu G. 2024. Statistical physics investigation on the simultaneous adsorption mechanism of Cd^{2+} and Pb^{2+} on amino functionalized activated carbon derived from coal gasification fine slag. *Journal of Environmental Chemical Engineering*, 12, 1–12. <https://doi.org/10.1016/j.jece.2024.112635>
33. Liu H., Mo Z., Li L., Chen F., Wu Q., Qi L. 2017. Efficient removal of copper(II) and malachite green from aqueous solution by magnetic magnesium silicate composite. *Journal of Chemical & Engineering Data*, 62(10), 3036–3042. <https://doi.org/10.1021/acs.jced.7b00041>
34. Livani M.J., Ghorbani M., Mehdipour H. 2018. Preparation of an activated carbon from hazelnut shells and its hybrids with magnetic $NiFe_2O_4$ nanoparticles. *New Carbon Materials*, 33(6): 578–586. [https://doi.org/10.1016/S1872-5805\(18\)60358-0](https://doi.org/10.1016/S1872-5805(18)60358-0)
35. Majdi H.S., Jaafar M.S., Abed A.M. (2019). Using KDF material to improve the performance of multi-layers filters in the reduction of chemical and biological pollutants in surface water treatment. *South African Journal of Chemical Engineering*, 28, 39–45. <https://doi.org/10.1016/j.sajce.2019.01.003>
36. Mi Y., Wang W., Zhang S., Guo Y., Zhao Y., Sun G., Cao Z. (2024). Ultra-high specific surface area activated carbon from Taihu cyanobacteria via KOH activation for enhanced Methylene blue adsorption. *Chinese Journal of Chemical Engineering*, 67, 106–116. <https://doi.org/10.1016/j.cjche.2023.12.002>
37. Mollaei M., Karbasi F., Haddad A.S., Baniasadi H. (2024). Fabrication of biocomposite materials with polycaprolactone and activated carbon extracted from agricultural waste. *Colloids and Surfaces A: Physicochemical and Engineering Aspects*, 702(2), 1–14. <https://doi.org/10.1016/j.colsurfa.2024.135175>
38. Moussa S.I., Ali M.M.S., Sheha R.R. (2021). The performance of activated carbon/ $NiFe_2O_4$ magnetic composite to retain heavy metal ions from aqueous solution. *Chinese Journal of Chemical Engineering*, 29, 135–145. <https://doi.org/10.1016/j.cjche.2020.07.036>
39. Musa S.A., Abdulhameed A.S., Baharin S.N.A., AlOthman Z.A., Selvasembian R., Jawad A.H. (2024). Pyrolyzed coal base high surface area and mesoporous activated carbon for methyl violet 2B dye removal: Optimization of preparation conditions and adsorption key parameters. *Chemical Engineering Research and Design*, 205, 67–78. <https://doi.org/10.1016/j.cherd.2024.03.015>
40. Njewa J.B., Vunain E., Biswick T. (2022). Synthesis and characterization of activated carbons prepared from agro-wastes by chemical activation. *Journal of Chemistry*, 2022, 1–13. <https://doi.org/10.1155/2022/9975444>
41. Oladimeji T.E., Odunoye B.O., Elehinafe F.B., Obanla O.R., Odunlami, O.A. (2021). Production of activated carbon from sawdust and its efficiency in the treatment of sewage water. *Heliyon*, 7, 1–6. <https://doi.org/10.1016/j.heliyon.2021.e05960>
42. Qasem N.A.A., Mohammed R.H., Lawal D.U.

- (2021). Removal of heavy metal ions from wastewater: a comprehensive and critical review. *NPJ Clean Water*, 4(36), 1–15. <https://doi.org/10.1038/s41545-021-00127-0>
43. Riyanti R., Hariani P.L., Purwaningrum W., Elfita E., Damarril S.S., Amelia I. (2018). The synthesis of MnFe_2O_4 -activated carbon composite for removal of Methyl red from aqueous solution. *Molekul*, 13(2), 123–132. <http://dx.doi.org/10.20884/1.jm.2018.13.2.435>
44. Saad F.N.M., Quana O.C., Izhara T.N.T., Hwidi R.S., Syafiuddin A. (2024). Evaluation of the use of activated carbon derived from coconut shells to treat car wash wastewaters. *Desalination and Water Treatment*, 319, 1–5. <https://doi.org/10.1016/j.dwt.2024.100452>
45. Shabir S., Hussain S.Z., Bhat T.A., Amin T., Beigh, M., Nabi S. (2024). High carbon content microporous activated carbon from thin walnut shells: Optimization, physico-chemical analysis and structural profiling. *Process Safety and Environmental Protection*, 190, 85–96. <https://doi.org/10.1016/j.psep.2024.06.121>
46. Shaida M.A., Dutta R.K., Sen A.K., Ram S.S., Sudarshan M., Naushad M., Boczkaj G., Nawab M.S. (2022). Chemical analysis of low carbon content coals and their applications as dye adsorbent. *Chemosphere*, 287(4), 1–16. <https://doi.org/10.1016/j.chemosphere.2021.132286>
47. SNI No. 06-3730-1995. Arang aktif teknis. Badan Standarisasi Nasional-BSN, Indonesia
48. Sun G., Zhang J., Li, X., Hao B., Xu F., Liu K. (2023). Self-assembled morphology-controlled hierarchical Fe_3O_4 @LDH for Cr(VI) removal. *Journal of Environmental Chemical Engineering*, 11(3), 1–11. <https://doi.org/10.1016/j.jece.2023.110129>
49. Tahmasebpour R., Peighambardoust, S.J. (2024). Decontamination of tetracycline from aqueous solution using activated carbon/ Fe_3O_4 /ZIF-8 nanocomposite adsorbent. *Separation and Purification Technology*, 343, 1–11. <https://doi.org/10.1016/j.seppur.2024.127188>
50. Vaithianathana R., Anitha P., Sudha R., Ramachandran A. (2023). Equilibrium and kinetic studies on the removal of cadmium(II) by Fe_3O_4 loaded activated carbon prepared from castor seed shell. *Desalination and Water Treatment*, 306, 75–88. <https://doi.org/10.5004/dwt.2023.29779>
51. Vunain E., Masoamphambe E.F., Mpeketula P.M.G., Monjerezi M., Etale A. (2019). Evaluation of coagulating efficiency and water borne pathogens reduction capacity of *Moringa oleifera* seed powder for treatment of domestic wastewater from Zomba, Malawi. *Journal of Environmental Chemical Engineering*, 7(3), 1–8. <https://doi.org/10.1016/j.jece.2019.103118>
52. Yang C., Florent M., de Falco G., Fan H., Bando-sz T.J. (2020). ZnFe_2O_4 /activated carbon as a regenerable adsorbent for catalytic removal of H_2S from air at room temperature. *Chemical Engineering Journal*, 394, 1–11. <https://doi.org/10.1016/j.cej.2020.124906>